DALTON
FULL PAPER

Four-co-ordinated copper(II) species obtained by X-ray irradiation of a three-co-ordinated copper(I) complex: a single crystal EPR study

Cornelia G. Palivan *† [a] and Sundara Ramaprabhu [b]

[a] *Department of Atomic and Nuclear Physics, Faculty of Physics, University of Bucharest, Bucuresti-Magurele, P.O. Box MG-11, Romania*
[b] *Department of Physics, Indian Institute of Technology, Madras, India*

Received 31st May 2000, Accepted 21st August 2000
First published as an Advance Article on the web 22nd September 2000

X-Ray irradiation of a single crystal of chlorobis(1-isopropylimidazolidine-2-thione)copper(I) led to the formation of two copper(II) species whose structures were studied by EPR spectroscopy. The EPR parameters provide information on the structural changes which characterize the formation of the four-co-ordinated copper(II) species when the three-co-ordinated copper(I) precursor reacts with radiogenic radicals formed during the irradiation and provide insight into the reaction mechanism.

Introduction

The complexes of copper cations, both mono- and di-valent, exhibit a wide variety of structural features, leading to important practical consequences.[1] In particular it is probably an essential factor for many of the properties of copper-containing enzymes: when these enzymes participate in redox reactions the Cu atom switches between the Cu(I) and Cu(II) states.[2,3] These electronic changes are accompanied by reorganizations in the first ligand sphere and/or co-ordination number.[3,4] The paramagnetism of the copper(II) cation and the sensitivity of the spectral parameters to the stereochemistry of the surrounding ligands make EPR a tool of choice for the study of such systems.[5]

A further field where the variable stereochemistry of copper cations plays an important role and where useful information may be obtained from EPR spectra is that of radiation-induced damage in solids.[6] All such processes produce lattice imperfections, *i.e.* changes in the crystal microstructure. The displaced atoms are ionized, and are therefore rapidly decelerated and come to rest in interstices, producing two types of point defects, vacancies and interstitial atoms. Thus ionizing radiation provides an effective route to paramagnetic electron-gain and loss species suitable for EPR studies which give important insight into the structures of the centres, often not accessible by other techniques.[6]

The present study characterizes the copper(II) species yielded by molecular transformations which occur when the three-co-ordinated complex chlorobis(1-isopropylimidazolidine-2-thione)copper(I) complex, **1**, reacts with radiogenic radicals formed during irradiation. This type of compound, where the X-ray irradiation results in transformation of a three-co-ordinated copper(I) complex into a four-co-ordinated copper(II) complex,[7] is reminiscent of a model used for describing the type I copper(II) active site in blue proteins.[3,8] For this reason the analysis of the EPR tensors which characterise the first co-ordination sphere around the copper ion in the paramagnetic species and its relations with the molecular axes in the undamaged molecule will provide insight to this transformation. The lattice effects prevent one from extending the results obtained in the solid state to the liquid state, where other mechanisms may be important.

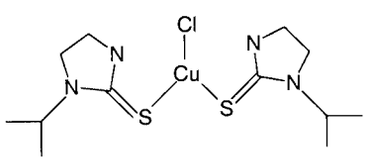

Experimental

Sample preparation

Complex **1** was prepared as previously reported.[9] A single crystal of it was obtained by slow evaporation of a $C_2H_4Cl_2$ solution in a N_2 atmosphere, at 295 K. This was then irradiated for 1.5 hours at room temperature by using an X-ray tube with a tungsten anticathode (30 mA, 30 kV).

EPR measurements

The EPR spectra were recorded at room temperature on a JEOL JES ME-3X spectrometer (X band, 100 kHz field modulation). The irradiated single crystal was glued to a small perspex cube in such a way as to permit rotation of the sample around the three orthogonal axes of a referential OX, OY, OZ, aligned along the *a*, *b*, *c* crystallographic axes respectively. The angular dependence of the spectra was analysed by taking into account the electronic and nuclear Zeeman interactions, the hyperfine interaction with $^{63/65}$Cu as well as the hyperfine interaction with ligands having $I \neq 0$ (up to three different types of ligands), eqn. (1), where μ_B is the Bohr magneton and μ_N the nuclear magneton, S and I correspond to the electron and

$$\boldsymbol{H} = \mu_B \vec{S}\hat{g}\vec{B} - \mu_N \sum_i g_i \vec{B}\vec{I}_i + \vec{S}\hat{A}\vec{I} + \sum_i \vec{S}\hat{A}_i\vec{I}_i \qquad (1)$$

nuclear spin respectively, and $\vec{B}$ represents the magnetic field vector. The first term describes the electronic Zeeman effect, with $\hat{g}$ the gyromagnetic tensor, the second represents the nuclear Zeeman effect, and the last two express the hyperfine and superhyperfine interactions, with the hyperfine/superhyperfine tensors $\hat{A}_i$. The various tensors were obtained by using a second order perturbation treatment combined with a Simplex/Migrad (Minuit version) minimization algorithm.[10]

The simulations of the spectra or parts of them were performed by using a locally developed program (FFT algorithm with Gaussian line shape for the signals), taking into account the natural abundance of $^{63/65}$Cu and $^{35/37}$Cl atoms. For some

† Present address: Institute for Physical Chemistry, University of Basel, Klingelbergstrasse 80, 4056 Basel, Switzerland. E-mail: Cornelia.Palivan@unibas.ch

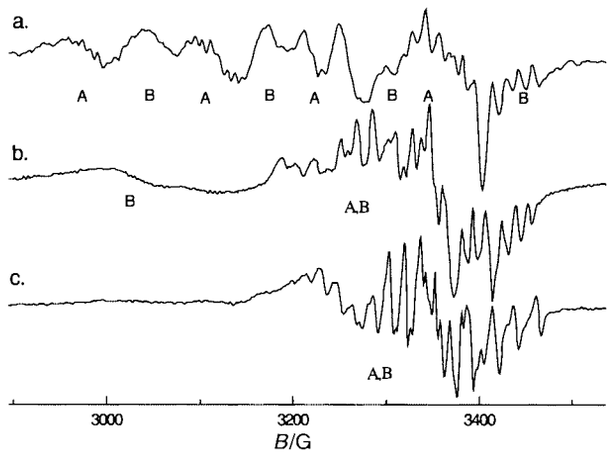

Fig. 1 Experimental EPR spectra obtained from an X-irradiated crystal of complex **1** with the magnetic field aligned along the *a* axis direction (a), the *b* axis direction (b) and the *c* axis direction (c).

orientations the signal positions were calculated by using a seventh-order perturbation algorithm. The bonding coefficients were calculated from EPR data, by using a simple semi-empirical LCAO-MO scheme, originally introduced by Maki and McGarvey[11] that expresses anisotropic *g* values and hyperfine constants as functions of molecular-orbital coefficients. Furthermore the spin densities in ligand orbitals have been calculated. They describe the delocalization of the unpaired electron into the first sphere of ligands co-ordinated with the copper ion.

Results

Complex **1**, whose crystal structure has been previously published,[9] is orthorhombic (space group *Pbca*). The arrangement of the molecules in the crystal structure permits the migration of small molecular fragments to a nearby copper center.

The EPR spectra obtained after the irradiation of complex **1** indicate the formation of stable paramagnetic species trapped in the single crystal at room temperature. The spectra are difficult to analyse for the following reasons: (a) the presence of two types of paramagnetic centers (**A**, **B**), the separate signals being observed only for some orientations; (b) the contribution of both isotopes ^{63}Cu and ^{65}Cu; and (c) the presence of magnetically non-equivalent orientations of the paramagnetic species ("site splitting").

Fig. 1 shows the EPR spectra obtained with the magnetic field aligned along the directions of the crystallographic axes. For these orientations all molecules of the same paramagnetic species are magnetically equivalent, which makes it possible clearly to distinguish the presence of two types of resonances **A**, **B**, assigned to different paramagnetic species (Fig. 1a,b). The angular variation of the EPR signals is again proof for the presence of two different types of species. They are especially well characterized by: (a) a pattern of four sets of lines clearly distinguished in the *ac* and *ab* planes and which characterize the species **A** (Fig. 2b,c); (b) a pattern of four sets of lines which can be distinguished only at crystal orientations where the sets from species **A** are sufficiently separated; this pattern characterizes the species **B** (Fig. 2a,c). For both paramagnetic species the four sets of lines correspond to the four values of M_I associated with the nuclear spin of Cu. The additional hyperfine structure present in each set reveals the presence of several ligand nuclei with $I \neq 0$ linked to the copper ion.

In accordance with the crystal symmetry two sets of patterns (each containing four sets of signals) are obtained in all three rotation planes due to the magnetically inequivalent sites (for both **A** and **B** species). Even if the spectra become particularly complex in certain regions of all three planes, it is still possible

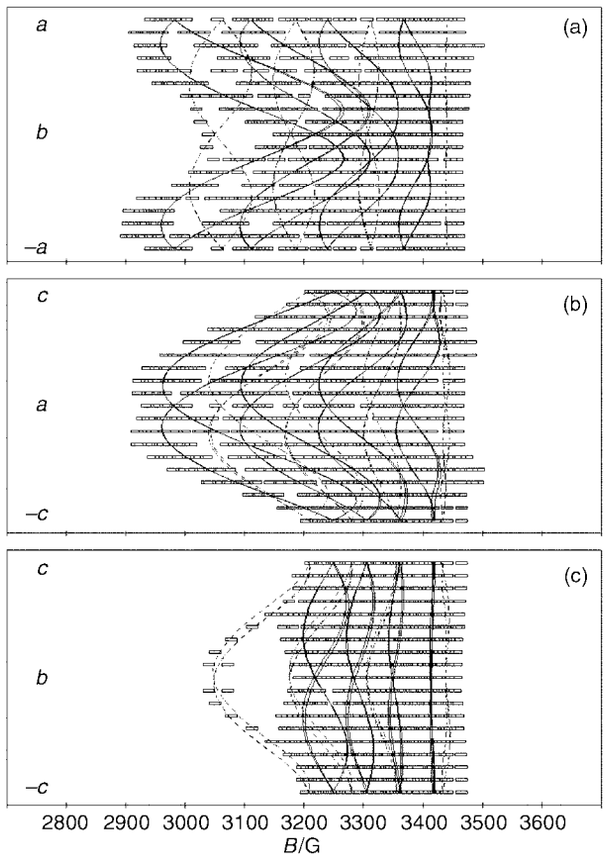

Fig. 2 Angular variations of the EPR signals obtained with an X-irradiated crystal of complex **1**. The curves have been calculated by using the gyromagnetic and ^{63}Cu hyperfine tensors given in Table 1 for the species **A** (dashed lines) and species B (dotted lines) for two magnetically non-equivalent sites. The magnetic field lies in the *bc* plane, (a), in the *ac* plane (b) or in the *ab* plane (c).

to recognize the four hyperfine copper sets of resonances for species **A**, whose signals are more intense than those of **B**. For the second species, only the copper sets of low and high magnetic field are well enough separated from those of **A**, in large regions of the *bc*, *ab* planes. The four hyperfine copper sets of species **B** can be observed only for some orientations in the *ac* and *bc* planes (for example Fig. 1a).

In order to analyse the superhyperfine structure corresponding to species **A**, the interaction with two Cl atoms was considered in a manner identical to that previously reported,[12] for a CuS_2Cl_2 fragment. The chlorine hyperfine interaction was determined by simulating the structure of the low-field set in the regions where both species and both sites do not overlap (regions M in Fig. 3). As an example, the simulation of the low-field set (Fig. 4) was obtained by assuming that the chlorine atoms are quasi-equivalent for this orientation (*** in Fig. 3: 40° away from $-c$ axis, in the *ac* plane). The simulation takes into account both ^{63,65}Cu and ^{35,37}Cl in their natural isotopic abundance.

The results of the simulation procedure for the regions where there is no overlap were used as input data for the minimization algorithm for obtaining the chlorine hyperfine tensors. For the regions where the signals overlap it was not possible to simulate the spectra with sufficient accuracy due to the number of transitions and to the remarkably narrow linewidth (<2 G) which makes the intensities very sensitive to the choice of parameters and line shape. For this reason the various tensors that characterize the species **A** were obtained in a double step minimization procedure: (a) *g* and copper hyperfine tensors were obtained by using the Minuit optimization program for the central position of the four sets of lines; (b) the input data for chlorine hyperfine interaction were added into the minimization procedure in

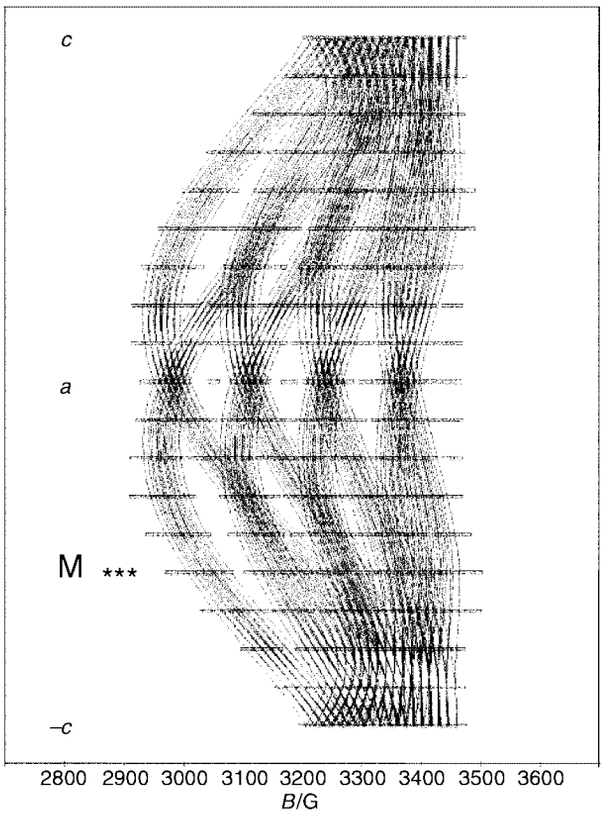

Fig. 3 Angular variations of the EPR signals obtained with an X-irradiated crystal of complex **1**. The curves have been calculated by using the various tensors given in Table 1 for species **A**. The magnetic field lies in the *ac* plane. The low field part of the spectrum was simulated in the region marked M.

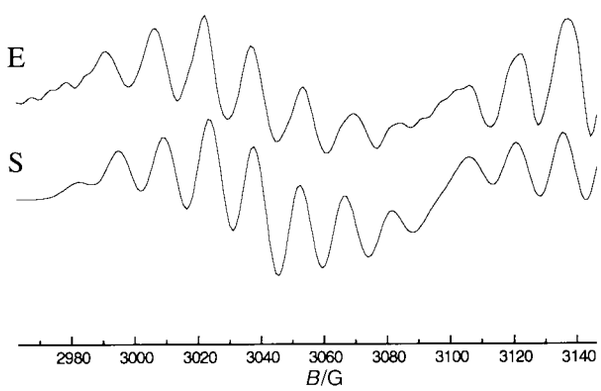

Fig. 4 Experimental (E) and simulated (S) EPR spectra (assuming two Cl atoms with $A_{Cl(1)} = 15.31$ and $A_{Cl(2)} = 12.89$ G) for the $M_I = -3/2$ line for Cu^{2+} in the *ac* plane, 40° away from *–c* (see Fig. 3 ***). The simulation takes into account Cu and Cl in natural isotopic abundance.

order to obtain the *g* tensor and hyperfine tensors for copper and chlorine atoms. In this procedure the hyperfine tensor for one of the chlorine atoms (b) was obtained with a rather poor precision due to the error in the determination of its coupling constants, in the planes where there is a considerable overlap of the signals. The various tensors corresponding to species **A** are presented in Table 1, and Fig. 3 shows the angular variation in the *ac* plane, obtained with the previously mentioned parameters, taking into account the magnetically inequivalent sites. In order to have a clear view of the signal positions only the ^{63}Cu and ^{35}Cl isotopes are presented.

In order to analyse the superhyperfine structure of species **B**, the pattern existing in the region of the high-field domain (which is distinct from species **A** over a large domain in the *ac* and *ab* planes) as is shown in (Fig. 2b,c) has to be taken into account. It indicates that an interaction with only one nucleus

Table 1 Spin Hamiltonian tensors for the copper(II) paramagnetic species trapped in an X-irradiated single crystal of complex **1**

	Eigenvectors		
	X	*Y*	*Z*
Species **A**			
g tensor			
2.034	0.321	−0.245	−0.915
2.044	−0.120	0.948	−0.296
2.171	−0.939	−0.205	−0.275
$A(^{63}Cu)$ tensor [MHz]			
(−)40.94	0.345	−0.184	−0.920
(−)48.24	−0.344	0.887	−0.306
(−)136.25	−0.873	−0.422	−0.243
$A(^{35}Cl_1)$ tensor [MHz]			
5.39	−0.621	0.681	0.388
10.55	0.734	0.679	−0.017
15.72	0.275	−0.274	0.922
$A(^{35}Cl_2)$ tensor [MHz]			
7.31	0.662	−0.421	0.619
14.26	−0.749	−0.349	0.564
17.22	0.021	0.837	0.547
Species **B**			
g tensor			
2.042	−0.401	−0.172	0.899
2.091	−0.565	−0.726	−0.391
2.130	−0.721	0.665	−0.194
$A(^{63}Cu)$ tensor [MHz]			
(−)56.72	−0.396	−0.221	0.891
(−)117.00	−0.594	−0.678	−0.432
(−)143.63	−0.700	0.700	−0.137

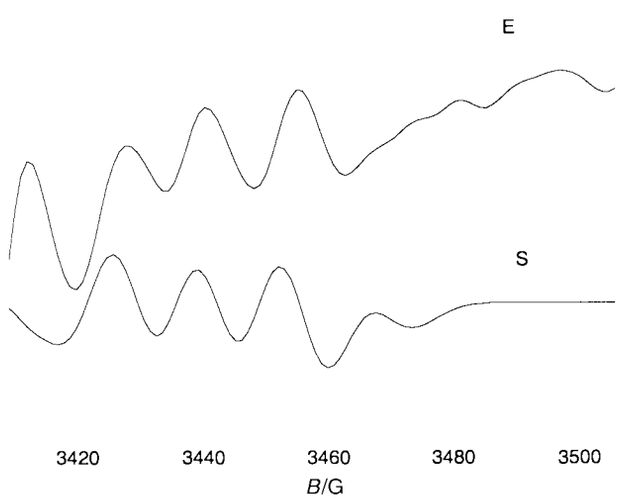

Fig. 5 Experimental (E) and simulated (S) EPR spectra (assuming one Cl atom with $A_{Cl} = 20.40$ G) for the $M_I = 3/2$ line for Cu^{2+} in the *ab* plane and the magnetic field aligned along *a* axis direction. The simulation takes into account Cu and Cl in natural isotopic abundance.

with $I = 3/2$ needs to be considered. The high-field set of lines was simulated in the regions where there is no overlap from the high-field set of lines of **A** (the region around the *a* axis in the *ab* or *ac* planes). An example of the simulation of the high-field set for species **B** is presented in Fig. 5 and corresponds to the high-field part of the spectra shown in Fig. 1a. The intensity of the four lines in the high-field set of species **B** is affected by the ^{65}Cu isotope high-field set from **A** and for this reason only the position of the lines was considered. The value of 58 MHz for the coupling obtained from the simulation of the

Table 2 Angular relations between some eigenvectors measured for the copper(II) paramagnetic species and some molecular directions measured for the undamaged copper(I) complex (angles in °)

(a) Species **A**	Direction			
	g_{zz}	$A_{zz}(^{63}Cu)$	$A_{zz}(^{35}Cl_a)$	$A_{zz}(^{35}Cl_b)$
Cu–Cl bond	69	71	34	42
"N"	30	28	72	83

(b) Species **B**	Direction		
	g_{zz}	$A_{zz}(^{63}Cu)$	$A_{zz}(^{35}Cl_1)$
Cu–Cl bond	88	92	—
"N"	36	38	—

superhyperfine structure of the high-field part of the spectra has the same order of magnitude as the A_{zz} coupling for the chlorine atoms in species **A** and together with the fact that I = 3/2 leads us to suppose that the ligand responsible for the superhyperfine structure is a chlorine atom. However, even if the simulations are fairly accurate in the region mentioned, an unequivocal superhyperfine tensor for the Cl atom could not be obtained because of superposition of both patterns in the *bc* plane.

The gyromagnetic and ^{63}Cu hyperfine tensors of species **B** were obtained in a similar manner to those of **A**, and are shown in Table 1.

Since the EPR spectra of the various magnetically inequivalent sites for both **A** and **B** species coalesce when the magnetic field is oriented along the symmetry reference axes, there are two different possibilities for matching the curves. We report in Table 1 the tensors which lead to the best agreement between experimental and calculated signal positions.

The changes of the molecular structure during the irradiation were analysed by using characteristic orientations obtained from the eigenvectors, with respect to special directions in the initial copper(I) molecule (the original Cu–Cl bond direction, the direction of the normal to the plane containing Cl, Cu and S atoms) (Table 2).

Assuming the EPR parameters from Table 1 and using the semiempirical approach of Maki and McGarvey[11] for copper(II) complexes, it is possible to use a simple LCAO-MO scheme and express anisotropic g values and hyperfine constants as functions of molecular orbital coefficients and certain atomic constants. For copper, the general symmetry usually corresponds to an octahedral structure with tetragonal, rhombic or tetrahedral distortion which can arise from differences in donor atoms of the ligand or steric repulsion between chelating molecules. In our case the analysis of the angles between the principal axis of the hyperfine tensors of Cu and Cl, and special directions in the initial molecule (see Table 2), showed a considerable rearrangement of the bond directions. For this reason a low symmetry characterizes the first sphere of co-ordination around the copper ion for both paramagnetic species. We consider a rough estimation of the spin delocalization on the metal orbitals by taking into account a D_{2h} symmetry,[13] which represents the limiting case for a square planar arrangement.

In order to obtain more insight into the structure of the paramagnetic species **A** we consider the unpaired electron density distribution among the chlorine orbitals from the superhyperfine parameters. The principal superhyperfine values may be broken down into an isotropic component A_s, due to the contribution from the occupancy of the chlorine 3s orbital, and dipolar components due to the occupancy of the chlorine 3p orbitals. In the present situation both the chlorine $3p_z$ and $3p_x$ orbitals may overlap with the metal d orbital and give dipolar contributions A_{pz} and A_{px}. In addition a small dipolar contribution $A_{D'}$ from the unpaired electron density on the metal will occur and is estimated at ≈ 0.138 G.[14] Assuming that each interaction is due directly to the unpaired electron density in the orbital in question, all of these components are positive.

Table 3 Spin densities in the chlorine orbitals obtained from the hyperfine constants for the trapped copper(II) species **A**

Atom	Spin density f (%)				Spin density ratio
	3s	$3p_x$	$3p_z$	$3p_t$	f_s:f_p
Cl_a	0.75	2.32	4.76	7.08	0.11
Cl_b	0.91	3.10	4.62	7.72	0.12

By using the relations between the superhyperfine constants given in eqns. (2)–(4) and the components[15] above we obtain the

$$A_x = A_s + 2A_{px} - A_{pz} - A_D \quad (2)$$

$$A_y = A_s - A_{px} - A_{pz} - A_D \quad (3)$$

$$A_z = A_s + 2A_{pz} - A_{px} + 2A_D \quad (4)$$

fractional unpaired electron density in the chlorine 3s and 3p orbitals (Table 3).

Discussion

Species B

The primary radiogenic process is presumably the ionization of complex to produce the corresponding copper(II) cation. It is tempting to identify species **B**, which shows hyperfine structure arising from one copper nucleus and only one chlorine nucleus, with this primary product. The gyromagnetic and hyperfine tensors of **B** are not aligned, but make an angle of about 36° with respect to the direction of the normal direction to the CuSSCl plane in the undamaged molecule. The formation of the copper(II) species will almost certainly lead to a loss of planarity of the CuSSCl fragment and the directions of the resulting gyromagnetic and hyperfine tensors will thus be expected to deviate from the perpendicular to the molecular plane of the undamaged complex.

Species A

The g and ^{63}Cu hyperfine tensors have axial symmetry and they are again almost exactly aligned, the angle between the principal axes of the tensors being 1.9°. The values of the EPR parameters can be associated with a four-co-ordinated copper ion and the analysis of the superhyperfine structure of the spectra leads us to suppose a 2S2Cl first sphere of co-ordination around the copper ion (Fig. 4). The presence of the two chlorine atoms in the co-ordination sphere increases the ionicity within the unit cell, thereby increasing the g_{zz} value from the maximum 2.13, corresponding to 4S co-ordination,[16] to a value of 2.17 which is characteristic of 2S2Cl co-ordination.[12]

The formation of the four-co-ordinated species implies a rearrangement of the structure around the copper ion from a trigonal symmetry when the three-co-ordinated copper(I) complex is irradiated. Between the two limiting symmetries, square planar and tetrahedral, all combinations formed by mixing them in different ratios can exist.[17] It is well established that tetrahedral distortion of a square planar geometry is accompanied by a decrease of $A_{\parallel}$ and an increase of $g_{\parallel}$.[18] Thus, the values of the EPR parameters as well as the angles of the principal tensor axis with respect to special directions in the undamaged molecule can be used to establish the geometry of the co-ordination sphere around the copper ion.

The values of the EPR parameters (Table 1) are closer to the specific values for square planar than for tetrahedral symmetry,

as was established for other model compounds for copper proteins.[19] The angles between g_{zz} (respectively A_{zz} for ^{63}Cu) and the normal (N) to the plane formed by $ClCuS_1S_{01}$ atoms suggest a small tetrahedral distortion of the square planar symmetry around copper ion. The presence of this distortion is underlined by the values of the angles between chlorine A_{zz} directions (for both atoms) and the normal N, based on the fact that the A_{zz} axis lies in the direction of the Cl–Cu bond.[15] This is emphasized by the larger probability of changing the position of the chlorine atoms with respect to the initial molecule, than that of the molecular fragments containing sulfur atoms.

The A_{zz} of the chlorine nucleus, whose eigenvectors are determined with a good precision (Cl_a), makes an angle of 34° with respect to the Cu–Cl bond direction in the undamaged molecule. If we suppose that the A_{max}(Cl) eigenvector is aligned along the Cu–Cl bond,[15] this implies that during the irradiation process the Cu–Cl bond has moved away from its initial direction and moreover does not remain in the original co-ordination plane since the normal, N, makes an angle of 71° with $A_{zz}(Cl_a)$. The angle between the A_{zz} axis of the second Cl atom and the special directions in the undamaged molecule can be associated with a *cis* position of the chlorine atom, which is also moved out of the initial plane of the molecule. This position can be correlated with the magnetic equivalence of both chlorine atoms in the *ac* and *ab* planes, as previously mentioned, and with the angle between the A_{zz} eigenvectors of both chlorine atoms (74°).

The absence of information about the position of the sulfur ligands in the copper(II) complex prevents us from describing the oxidation mechanism with precision. A possible process of species **A** formation is the capture of a chloride ion by the primary copper(II), product of irradiation, tentatively identified with **B** above, from a neighbouring undamaged species **1**.[12] The crystal structure[9] shows that neighbouring molecules of **1** are arranged with their Cu–Cl bonds in an antiparallel fashion, with only 5.38 Å between the Cu atom of one molecule and the Cl atom of its neighbour, thus facilitating the postulated transfer of the chloride ligand. The diamagnetic copper(I) fragment resulting from this capture would be expected to have a linear arrangement of the S–Cu–S fragment, as observed in bis(2,6-dimethylpyridine)copper(I) perchlorate.[20] The successful completion of the transformation probably must thus occur at a defect that would permit considerable rearrangement from the bent to the linear conformation of the S–Cu–S fragment, thus explaining the simultaneous presence of both species **A** and **B**.

The comparison of the g_{zz}/A_{zz} value for **A** (157.1 cm) ‡ with that of the previous copper(II) complex (147.3 cm)[12] shows that in the present case a greater distortion characterizes the first sphere of co-ordination around the copper ion.[21] The magnetic parameters obtained for **A** are in agreement with the values of $g_{zz} > g_{xx,yy} > g_e$, suggesting that the complex has a $d_{x^2-y^2}$ ground state, characteristic of square planar, square base pyramidal and octahedral stereochemistry.[22] The small value for g_{xx}, 2.04 is due to the sulfur co-ordination which can give rise to a lower g value, close to 2.00, even in a ground state different from d_{z^2}.

The considerable rearrangement which occurs when the second chlorine atom arrives perpendicular to the initial CuClSS plane leads to a distorted square planar geometry around the copper ion and not to a tetrahedral one as would be normal if we consider the nature of the ligands. This arrangement is connected with the W shape of this type of molecule as previously shown.[23]

Calculation of bonding parameters from the EPR data

A simple semiempirical LCAO-MO approach can be used to measure the extent of ionic bonding (α^2) and of the contact term (K) from the EPR parameters (Table 1). The term K is independent of the direction of the magnetic field and the maximum value is attained at an intermediate covalence α^2.[24] The K value for species **A**, 0.287, is consistent with a tetrahedral distortion of the symmetry around the metal ion because this type of distortion leads to 3d–4p hybridisation.[25] The distortion also explains the reduction of the anisotropic hyperfine term from the value of 0.43. The contribution of 4p orbitals is not as large as would be required to obtain the hyperfine constants and for this reason the covalency of the Cu–Cl bonds as well as the large spin–orbit coupling of the chlorine atoms have to be taken into account.[18] Furthermore, sulfur is known to form fairly covalent bonds with copper(II) and its spin–orbit coupling constant is fairly large, close to half the value of Cu(II).[26]

The terms comprising the factor α^2 arise from the dipole–dipole interaction between magnetic moments associated with the spin motion of the electron and the nucleus. This contribution is reduced by delocalization of the unpaired electron on the neighbouring atoms. Its value decreases with increasing covalency to a minimum theoretical value of 0.5 for a completely covalent copper–ligand bond and is equal to 1.0 for a completely ionic metal–ligand bond. The value obtained for species **A** is 0.70 which is normal for these types of ligands where the unpaired electron is considerably delocalized.

In order to describe the unpaired electron density distribution among the chlorine orbitals the relations between the isotropic and dipolar terms are used. The values from Table 3 suggest a s:p orbital occupancy ratio of about 0.1:1 and the unpaired electron spends about 8% of its time on Cl_a and about 9% on Cl_b, a situation which indicates that the bonding is primarily between metal 3d and chlorine 3p orbitals.

When the overlap of the metal orbitals with the ligand orbitals is taken into account, we find that the unpaired electron population of the sulfur orbitals is approximately 17%, consistent with previously analysed copper(II) species with 2Cl2S first sphere co-ordination.[12]

Conclusion

The present study gives clear evidence that a square planar tetrahedrally distorted copper(II) species is formed by X-ray irradiation of the three-co-ordinated copper(I) complex, which involves capture of a neighbouring chloride ion and a considerable rearrangement of the molecule to accommodate a four-co-ordinated environment around the copper ion. This mechanism of structural change is similar to the redox mechanism of the type I copper(II) site in blue proteins which can be considered as an intermediary species in the structural pathway between the trigonal planar copper(I) geometry and the compressed tetrahedral copper(II) geometry. A second species is tentatively identified as a three-co-ordinated copper(II) complex, presumably the primary ionization product of the copper(I) derivative.

Acknowledgements

C. G. Palivan thanks Professor E. A. C. Lucken, University of Geneva, for useful discussions concerning the structures and the processes involved in the formation of these types of copper complexes.

References

1 M. Pascaly, I. Jolk and B. Krebs, *Chem. Userer Zeit*, 1999, **33**, 334; B. G. Malmstrom and J. Leckner, *Curr. Opin. Chem. Biol.*, 1998, **2**, 286.
2 I. Solomon, L. B. La Croix and D. W. Randall, *Pure Appl. Chem.*, 1998, **70**, 799; K. Pierloot, J. O. A. De Kerpel, U. Ryde, M. H. M. Olsson and B. O. Roos, *J. Am. Chem. Soc.*, 1998, **120**, 13156.
3 A. Messerschmidt, *Struct. Bonding* (*Berlin*), 1998, **90**, 37.
4 J. A. Gluckert, M. D. Lowery and E. I. Solomon, *J. Am. Chem. Soc.*, 1995, **117**, 2817.
5 A. E. Palmer, D. W. Randall, F. Xu and E. I. Solomon, *J. Am. Chem. Soc.*, 1999, **121**, 7138; J. R. Pilbrow, *Transition Ion Electron Paramagnetic Resonance*, Clarendon Press, Oxford, 1990.

‡ 1 cm ≡ 2.141969 G^{-1}, where 10 G = 1 mT.

6 M. R. C. Symons and D. X. West, *J. Chem. Soc.*, *Dalton Trans.*, 1985, 379; M. C. R. Symons, *Pure Appl. Chem.*, 1981, **53**, 223.
7 S. Ramaprabhu, *J. Mol. Struct.*, 1999, **478**, 29.
8 E. I. Solomon, M. D. Lowery, J. A. Gluckert and L. B. La Croix, *Adv. Chem. Ser.*, 1997, **253**, 317; M. H. M. Olsson, U. Ryde and B. O. Roos, *Protein Sci.*, 1998, **7**, 2659.
9 S. Ramaprabhu and E. A. C. Lucken, *Z. Naturforsch.*, *Teil A*, 1992, **47**, 125.
10 CERN Minuit 1994, M. Iwasaki, *J. Magn. Reson.*, 1976, **16**, 417.
11 H. Maki and B. R. McGarvey, *J. Chem. Phys.*, 1958, **29**, 31.
12 C. G. Palivan, T. Berclaz, M. Geoffroy, S. Ramaprabhu and G. Bernardinelli, *J. Chem. Soc.*, *Faraday Trans*., 1995, **91**, 2155.
13 C. G. Palivan, H. M. N. Palivan, B. A. Goodman and C. Cristescu, *Appl. Magn. Reson.*, 1998, **15**, 477.
14 G. F. Kokoszka, C. W. Reimann and H. C. Allen, *J. Phys. Chem.*, 1967, **71**, 121.
15 R. J. Deeth, M. A. Hitchman, G. Lehmann and H. Sachs, *Inorg. Chem.*, 1984, **23**, 1310.
16 U. Sakaguchi and A. W. Addison, *J. Chem. Soc.*, *Dalton Trans.*, 1979, 600.
17 B. J. Hathaway, in *Comprehensive Coordination Chemistry*, Pergamon Press, Oxford, 1987, vol. 5, pp. 728–734.
18 A. Bencini, D. Gatteschi and C. Zancini, *J. Am. Chem. Soc.*, 1980, **102**, 5234; I. Bertini, G. Canti, R. Grassi and A. Scozzafava, *Inorg. Chem.*, 1980, **19**, 2198.
19 F. Cristiani, F. Demaitn, F. A. Devillanova, A. Diaz, F. Isaia, V. Lippolis and G. Verani, *J. Coord. Chem.*, 1996, **38**, 113.
20 L. M. Englehardt, C. Patawatchi, A. H. White and P. C. Healy, *J. Chem. Soc.*, *Dalton Trans.*, 1985, 117.
21 G. Serratrice, El. Mazoukia, C. Beguin, A. Jeunet, S. Refait, P. Cheutemps and J. L. Peirre, *J. Chim. Phys.-Phys. Chim. Biol.*, 1994, **91**, 753.
22 B. J. Hathaway, *Struct. Bonding* (*Berlin*), 1984, **57**, 55.
23 S. Ramaprabhu, E. A. C. Lucken and G. Bernardinelli, *J. Chem. Soc.*, *Dalton Trans.*, 1995, 115.
24 A. Rockenbauer, *J. Magn. Reson.*, 1979, **35**, 429.
25 M. Sharnoff, *J. Chem. Phys.*, 1964, **41**, 2203; M. Sharnoff, *J. Chem. Phys.*, 1965, **42**, 3383.
26 B. Morosin and K. Lawason, *J. Mol. Spectrosc.*, 1964, **12**, 98; J. Ferguson, *J. Chem. Phys.*, 1964, **40**, 3406.